

# **Chapter 1 – The Basic Components of Seismo-Ionospheric Coupling**

## **1.1 Introduction**

During the last few years in the course of discussions with our colleagues on different scientific forums, and discussions with the referees of our journal papers we realized one very simple problem, which complicates the understanding of seismo-ionospheric coupling – it is lack of knowledge. The subject itself is multi-disciplinary, ranging from pure mechanics to space plasma physics, demanding simultaneous knowledge of many special disciplines such as plate tectonics, seismology, atmosphere and ionosphere physics and chemistry, and atmospheric electricity. Of course, the fields of seismology and ionosphere physics are very far one from another and discussions between representatives of these groups remind us of a discussion between the blind and the deaf. This entails a lot of unfounded conflicts and complications. The only answer we see is to familiarize those who really want to understand the problem at least with the basic ideas of the disciplines mentioned above. Of course, the seismologist who picks up our book probably should not read the paragraph devoted to seismology but we strongly recommend he looks through the other paragraphs, especially the ionospheric one.

We do not intend to cover all the principles of modern seismology, as well as other disciplines to be described in the first chapter. Our wish is to give newcomers the most important ideas which will be used in the following text discussing the problems of seismo-ionospheric coupling.

From the perspective of a discussion of the physical mechanisms of seismo-ionospheric coupling, we decided to include in the first chapter the following disciplines:

- Seismology
- Ionosphere physics and morphology
- Radiative troposphere plasmachemistry
- Atmospheric electricity

## 1.2 Seismology

Earthquake physics is a very complex and broad topic. It involves many scales of the Earth's crustal structure starting from tectonic plates and finishing with the microscopic processes involved in the friction, generation of electric charge and chemical reactions.

Earthquake occurrence is connected with the Earth's crustal dynamics. The Earth's crust is the rigid external shell of our planet consisting of the continental and oceanic crust. The thickness of the continental crust is of the order of 40 km and the oceanic one – is respectively near 6 km. The crust and the upper layer of the mantle form the lithosphere consisting of semi rigid plates of different sizes. The slow movement of these plates over the asthenosphere and ocean floor extension is called plate tectonics (Oreskes 2003). Collision of these plates leads to the diving of one plate edge under another (convergent or subduction boundaries). Subduction leads to the formation of different geological structures starting from the oceanic trench in the zone of plates contact, formation of new mountains and zones of volcanic activity. Apart from the subduction process there are other kinds of plate relative motion. Plate separation (divergent boundaries) generating the oceanic crust, and transform boundaries when plates move one along another as occurs at the San-Andreas fault in California. A simplified diagram of plate boundary configuration is presented in Fig. 1.1. All these movements lead to a strain accumulation within the Earth's crust, to mechanical deformations and crust rupture when the deformation exceeds the limit of mechanical strength. The process of rupture is the earthquake itself. It is natural to expect a difference in earthquake characteristics for every type of tectonic plate contact.

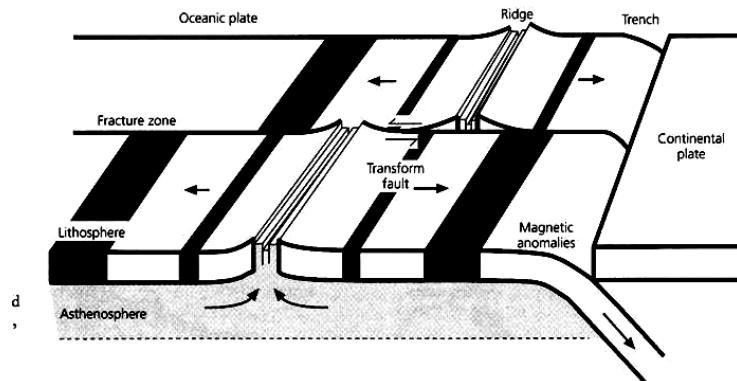


**Fig. 1.1** Schematic presentation of the different types of tectonic plate borders

Before we move on to the physical aspects of earthquakes, some introductory information is necessary. Those who are interested in more extended information can find this in recent monographs starting from elementary books (Bolt 1993;

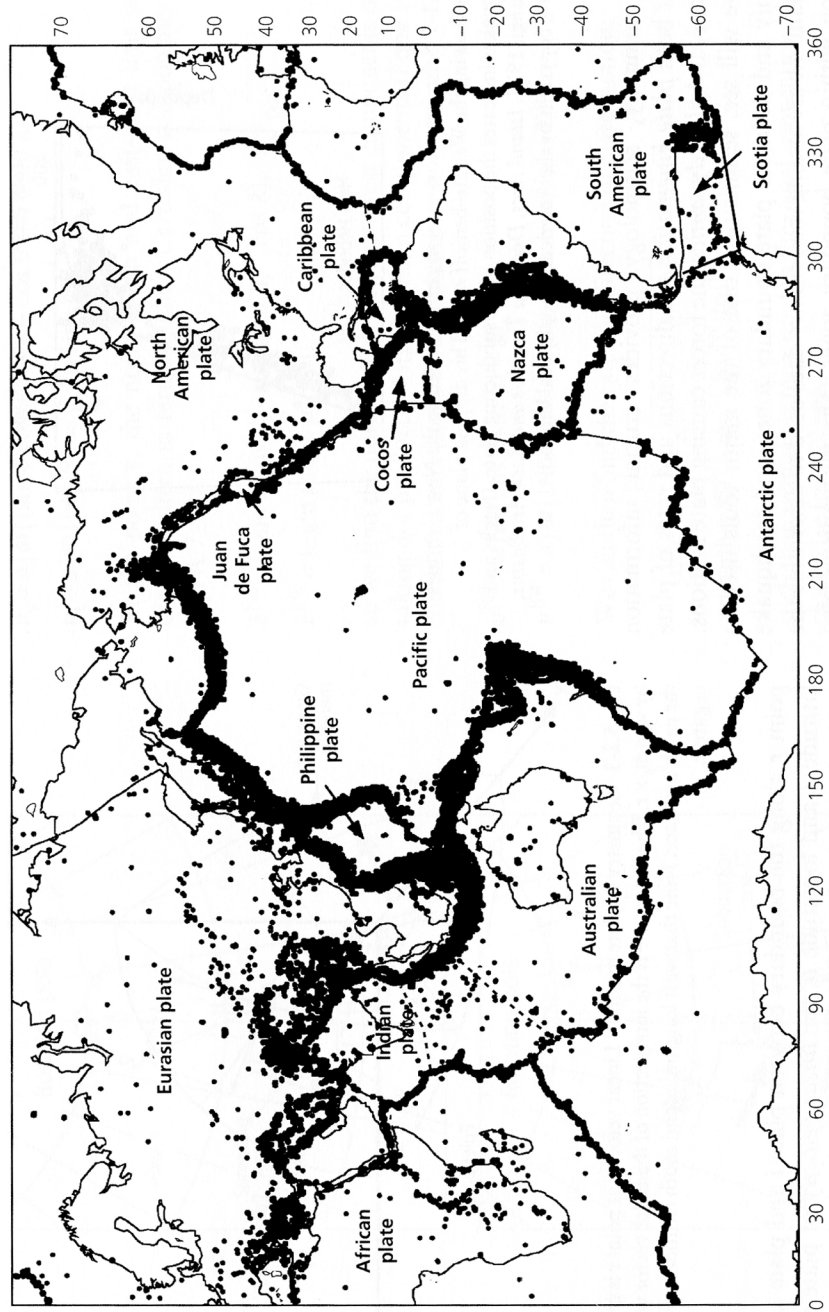
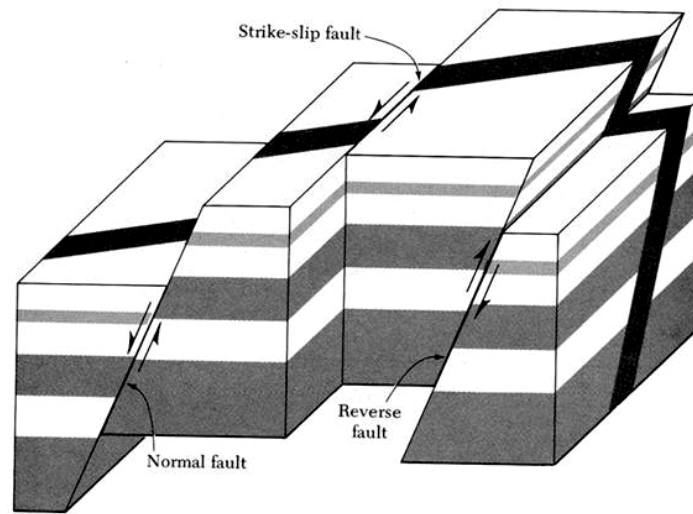


Fig. 1.2 Global earthquake seismicity in relation to the tectonic plate boundaries

Brumbaugh 1999) up to more advanced manuals (Shearer 1999; Stein and Wysession 2003). We strongly recommend the last one. Taking into account that earthquakes are the result of the tectonic plates contact, their global distribution is not uniform and is concentrated close to the tectonic plate's boundaries, which is demonstrated in Fig. 1.2. Except for the Himalayan region where the plate border is not obvious looking at the distribution of seismic activity, the other regions demonstrate a clear concentration of earthquakes on the tectonic plate borders.



**Fig. 1.3** The main types of tectonic fault geometry. Their combination is observed also

Fracturing of the Earth's crust has different scale sizes and in the more regional scale, it is associated with so-called tectonic faults (this is now generally expected). The conception of a fault was introduced by Anderson (1905) and he was the first who tried to explain the physics of faulting (Anderson 1942) by brittle fracture and applying the Coulomb criterion to this problem. Not all faults geometry could be explained by Anderson's theory, and it was developed and accomplished later by other investigators, but it is not our task to go deeply into faults mechanics – the only important conclusion we have is that the earthquakes occur on the fault – an existing discontinuity of the Earth's crust formed by the previous crustal movements. Additional information can be obtained in the monograph by Scholz (1990). From the mechanical point of view, the earthquake takes place when the applied stress exceeds the dynamic friction. The rupture criterion was introduced first by Griffith (1920). After the earthquake the dynamic friction becomes more than the stress on the rupture zone. If one takes two bricks and tries to move one in relation to another, you may find different types of relative movement. These relative movements of the fault walls (the main ones) are presented in Fig. 1.3.

The faults have also their hierarchy. Their length varies from thousands of kilometers (Anatolian and San Andreas Faults) up to local discontinuities of sev-

eral kilometers long. Usually after the earthquake a scarp is formed causing damage of mechanical constructions as one can see in Fig. 1.4 demonstrating damage along the fault of the recent catastrophic Chi-Chi earthquake in Taiwan on 21 September 1999 ( $M_w=7.6$ )



**Fig. 1.4** Top panel: the bridge damage and scarp of 8 m height formed along the fault of the Chi-Chi earthquake on the river floor. Bottom panel: the fault scarp passing across the racetrack of one of the schools in Puli, Taiwan

The earthquake's intensity is estimated from the oscillation created by different kinds of seismic waves (usually, the surface and body waves). The seismic waves are registered by seismographs and the largest vertical displacement  $A$  of the seismograph arrow was selected by Charles Richter in the 1930s to characterize the earthquake intensity by a parameter called the “local magnitude”  $M_L$  (Shearer 1999):

$$M_L = \log_{10} A + 2.56 \log_{10} \Delta - 1.67 \quad (1.1)$$

where  $A_0$  – is the amplitude of known reference event,  $\Delta$  – distance to the source of seismic wave. Here  $A$  is expressed in millimeters, and  $\Delta$  – in kilometers. After the Richter table providing  $A_0$  for different distances Bullen and Bolt (1985) proposed the empirical formula for  $M_L$ :

$$M_L = \log_{10} A(\Delta) - \log_{10} A_0(\Delta) \quad (1.2)$$

But this determination was very local because it depended on a specific place and was proposed for a specific instrument (Wood-Anderson seismograph), so development of a more universal parameter was necessary. Two other determinations of magnitude were proposed for two different types of seismic waves: the body wave named in seismology the P-wave, and the surface Rayleigh wave, named the S-wave. These waves have different propagation velocity, and different periods (the body wave period is smaller by order of magnitude in comparison with the surface wave). Taking into account the amplitude-frequency characteristic of the seismographs, one should expect that these magnitude definitions would be different which is the case. The body wave magnitude is expressed as:

$$m_b = \log_{10}(A/T) + Q(h, \Delta) \quad (1.3)$$

where  $T$  is the dominant period of the body waves, and  $Q$  again the empirical function depending on the range and the depth of the event. The surface wave magnitude will be expressed as:

$$M_s = \log_{10}(A/T) + 1.66 \log_{10} \Delta + 3.3 \quad (1.4)$$

Here again  $T$  is the dominant period but now of the surface wave which is usually of the order of 20 s.

In addition to the frequency dependence of the seismographs,  $m_b$  and  $M_L$  are exposed to the saturation effect for the strong earthquakes. In addition it was necessary to elaborate a more physical estimation of earthquake intensity. That's why Kanamori (1977) proposed the magnitude definition based on the seismic moment of the earthquake, which is a more physical estimation of the earthquake energy. Generally speaking, the seismic moment is a tensor but for simplified estimations one can use the scalar definition of the seismic moment:

$$M_o = \mu D A \quad (1.5)$$

where  $\mu$  is the shear modulus,  $D$  is the fault displacement, and  $A$  is the area of the fault. The Kanamori's definition of the moment magnitude looks like:

$$M_w = 2/3 \log_{10} M_0 - 10.7 \quad (1.6)$$

The variety of magnitude definition methods leads to the fact that one can find different magnitude values for the same earthquake in the literature. This is demonstrated in Table 1.1 (after Shearer 1999):

**Table 1.1. Some Big Earthquakes ( $M_0$  in  $10^{20}$  Nm)**

Date	Region	$m_b$	$M_S$	$M_w$	$M_0$
1992 June 28	Southern California	6.2	7.3	7.5	2
1906 April 18	San Francisco		8.2	7.9	10
1989 May 23	Macquarie Ridge	6.4	8.2	8.2	20
1994 June 9	Bolivia	7.0		8.2	26
1977 August 19	Indonesia		8.1	8.3	30
1957 March 9	Aleutian Islands		8.2	9.1	585
1964 March 28	Alaska		8.4	9.2	820
1960 May 22	Chile		8.3	9.5	2000

To give an idea how much energy is released during strong earthquakes and to imagine the relationship between the number and energy released by small, moderate, and strong earthquakes, it is worth taking a look at Fig. 1.5 and Table 1.2 (Stein and Wyssession 2003). One can see that the most destructive and dangerous earthquakes have a magnitude higher than 7.

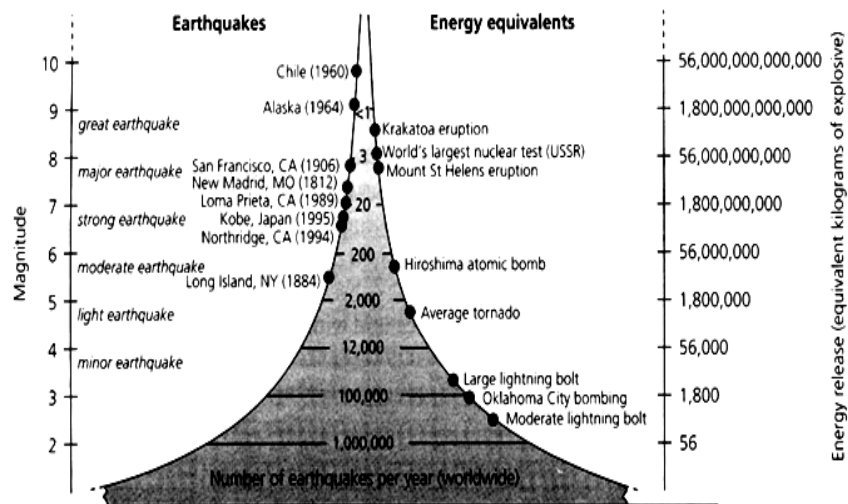


**Fig. 1.5** The number of events per year (horizontal axis), magnitude (*left axis*) and energy in trinitrotoluol equivalent (*right axis*) released yearly by Earth's seismic activity

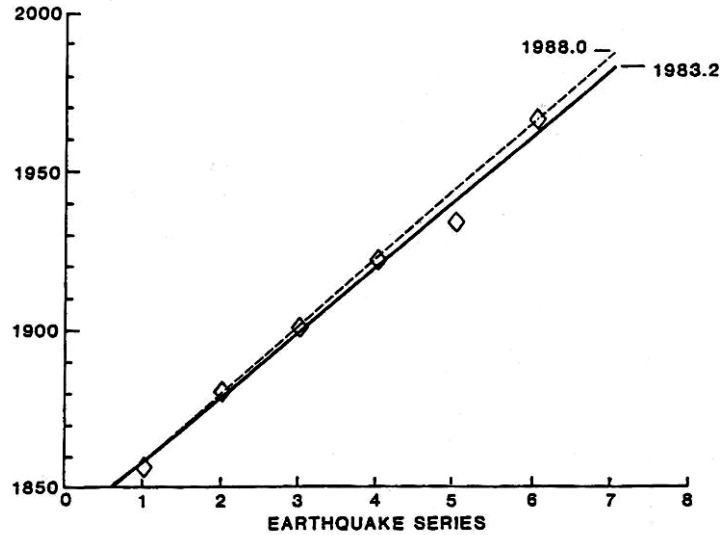


**Fig. 1.6** Regular periodicity of earthquakes with  $M \geq 6$  observed at Parkfield on San Andreas Fault

**Table 1.2.** Earthquakes number and energy released per year

Earthquake magnitude ( $M_s$ )	Number per year	Energy released ( $10^{15}$ J/yr)
$\geq 8.0$	0-1	0-1,000
7-7.9	12	100
6-6.9	110	30
5-5.9	1,400	5
4-4.9	13,500	1
3-3.9	>100,000	0.2

### 1.2.1 Physical Background of Earthquake Prediction

The classical approach to seismic prediction was based on the so-called seismic cycle implying the periodical storing and release of the seismic stress taking into account the continuous tectonic plate movement. This concept is usually connected with H. F. Reid who summarizing the mechanism of the California earthquake in 1906 published the theory of elastic rebound (Reid 1910). Turcotte and Spense (1974) made the calculations of periodicity for a homogeneous medium based on the elasticity theory. Of course, it is difficult to expect from the Earth's crust the ideal homogeneous structure but sometimes the earthquake sequence has



a strikingly regular periodicity which is demonstrated in Fig. 1.6 for the Parkfield earthquakes series. These comparatively simple conceptions were recently reconsidered from the point of view of the fast developing theory of fractals and chaos (Bak et al. 1988). The conception of self-organizing complex systems was put forward and described in the monograph by Rundle et al. (2000). But this approach, using pattern recognition techniques and self-organizing system theory, disregards the physical and chemical changes happening inside the fault and the seismic source. Our goal is just to consider the variations of different parameters observed before the earthquake.

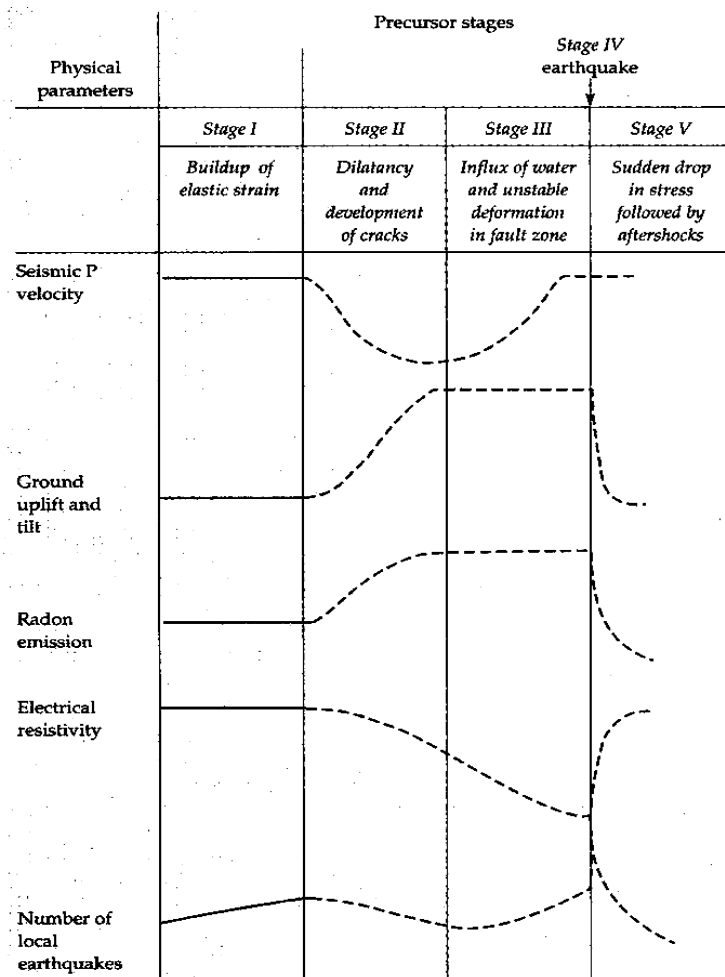


**Fig. 1.7** The precursory variations of different parameters within the interval of earthquake preparation

Abstracting from the earthquake forecast as an end in itself, we will pay more attention to the physics of the earthquake preparation process, especially its final stage. We will base this on the Scholz et al. approach (1973) regarding the earthquake preparation process and associated physical and chemical transformations within the Earth's crust in the zone of earthquake preparation. So we will take only one period of the seismic cycle to look how the fault transformation develops and what parameters manifest these changes. To have an idea of the seismic cycle stages we will use the picture from Bolt (1993), which is a slightly modified presentation of the Scholz picture, is used by many authors and presented here (Fig. 1.7). The basis of this approach relies on dilatation theory regarding crack formation within the Earth's crust and finally the formation of the main fault in the process of shallow earthquakes preparation. Actually, there were two models developed differing in the role of the underground water (Mjachkin et al. 1975). The process of earthquake preparation within one period of the seismic cycle was divided into five stages starting from the moment of the previous earthquake. Different physical parameters are traced. The first one (which actually put forward the dilatation theory) is the change of the P-wave velocity. The build of dilatation is detected by the velocity diminution in the second stage. Other precursors are ground uplift and tilt, radon emanation, electric resistivity and a number of small earthquakes within the area of earthquake preparation. Basing on present knowledge, we can say that these are not the only precursors registered. Most likely they are representatives of different groups of precursors, namely: mechanical deformation, geochemical and hydrological precursors, electromagnetic precursors, and naturally, the seismic ones. The stages of the cycle show the transition from the elastic deformation to a nonlinear process up to the rupture. The duration of the stages is variable depending on many factors that we will not discuss here. Our interest will concentrate mainly on stages III and IV, i.e. just before and during the earthquake. Some indirect data show that the final stage when the process becomes irreversible and the earthquake will take place, lasts at least several days.

We will not describe all types of precursors, for example, the water level changes or geoelectric potentials. One can find such descriptions in the literature (Rikitake 1976; Mogi 1985, Turcotte 1991; Bolt 1993; Lomnitz 1994; Uyeda et al. 2000). We concentrate mainly on the processes participating in the seismo-ionospheric coupling. It does not mean that some precursors are more important than others; simply the book's limits put restrictions on the items to be considered.

### **1.2.2 Radon Emanation as a Precursory Phenomenon**

Radon monitoring is one of the widely used techniques in geological studies. As is known, radon is the product of radium decay, which in turn appears after  $^{238}\text{U}$  decay. Radon is an ideal indicator in geological research because it is generated continuously in any geological structure. Its concentration loss due to decay (period of semi-decay is 3.825 days) and due to migration into the atmosphere is always compensated by new production. So the radon concentration in the given geological structure is more or less constant and is proportional to the uranium (radium)

content in the given massif. In the presence of cracks and upflowing gas streams the convective transport of the radon could be from the depths up to 200 m. There are no problems with the radon registration due to its high radioactivity. It is surely registered under 30 – 50 decays per second within one cubic meter, i.e. its activity is 3 – 50 Bk/m<sup>3</sup>

Radon migration is determined by the macroscopic diffusion coefficient which depends on the mode of geological structure deformation. It is obvious that under compression the diffusion coefficient decreases, and under unloading – increases. The loading-unloading process during earthquake preparation is the reason of the radon concentration variations before the earthquakes. Many authors reported radon variations before the earthquake and used them as a short-term earthquake precursor (Holub and Bready 1981; Segovia 1989; King et al. 1993; Utkin and Yurkov 1998; Garavaglia et al. 2000; Belyaev 2001). One can find a perfect review on the geochemical precursors of earthquakes in Toutain and Baurbon (1998). The example of the radon anomaly before the Kobe earthquake is presented in Fig. 1.8.

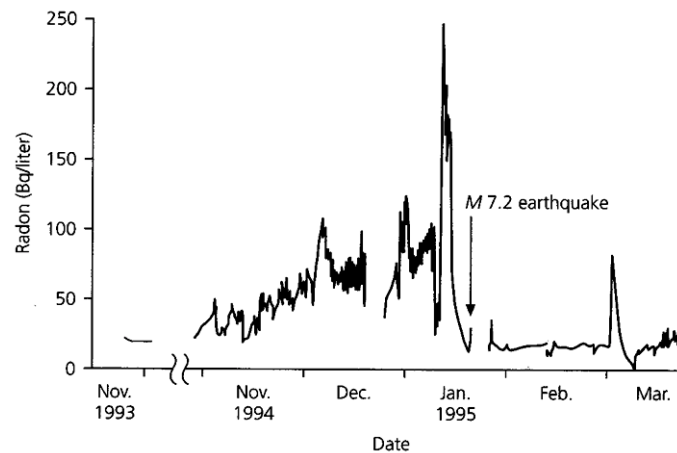


**Fig. 1.8** Radon in groundwater before and after the 16 January 1995, Kobe earthquake in Japan (Igarashi et al. 1995)

King et al. (1993) measuring the radon concentration in the area of tectonic faults in California have detected that the increase in radon concentration is observed not directly over the fault but some distance away. It coincides with the conception of Utkin and Yurkov (1998) who analyzed many cases of radon monitoring by different experimenters and came to the conclusion that radon variations have some regularities connected with the earthquake source. The epicenter of the future earthquake is, as a rule, inside the compression zone where radon concentration decreases before the earthquake (they called it the “near zone”). This near-zone radius for the earthquake with magnitude 5 is near  $24 \pm 15$  km. The size of the near-zone increases with the earthquake magnitude. The compression zone is surrounded by the stretching zone where the radon concentration growth

occurs before the earthquake. They named it the “far-zone” and determined its size as  $110 \pm 40$  km for an earthquake with magnitude 5. The problem of the distance where radon anomalies associated with earthquakes are measured will be discussed below.

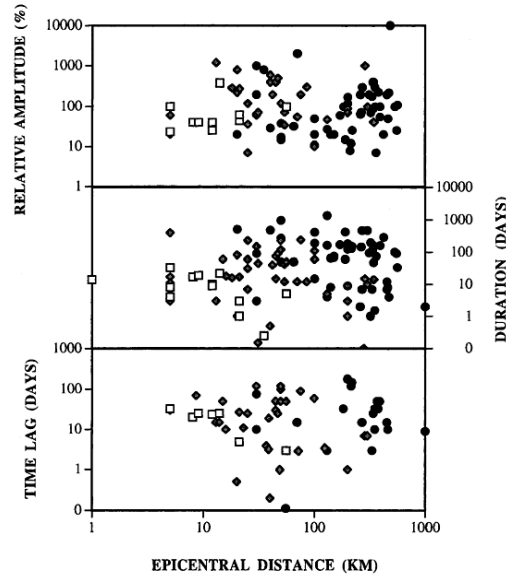


**Fig. 1.9** Plot of relative amplitudes (log scale), time lag (time between the onset of the anomaly and the related earthquake, in days) and duration (in days) of radon anomalies listed in Toutain and Baurbon (1999), review as a function of epicentral distances for selected magnitudes. *Dots*, *squares* and *lozenges* display earthquakes with magnitudes 0–3, 3–6 and 6–9, respectively. A general increase of maximum time lag and duration is seen with increasing epicentral distance

The radon concentration dynamic indicates the earthquake preparation process 3–4 months before the seismic shock with maximum dynamics registered 1–2 weeks before the event. The distance, time of advance and duration of radon anomaly growth with earthquake magnitude is shown in Fig. 1.9 (after Toutain and Baurbon 1999).

Besides its precursory value, we should attract the attention of the reader to the ionizing abilities of radon. It allows the creation of so-called “atmospheric plasma”. The atmospheric plasma conception will be discussed in the following paragraphs. Practically, radon is the first link in the chain of the physical processes providing the seismo-ionospheric coupling.

### 1.2.3 Other Geochemical Precursors

Earth degassing is more and more attracting the attention of scientists (King 1986; Wakita 1988; Toutain and Baurbon 1999; Heinicke et al. 2000; Taran et al. 2001). Furthermore, some recent ideas suggest that gas emanation is not the result of strength storing in the Earth's crust but is its reason (Iudin et al. 2002). These ideas develop the conception of gas convection (not diffusion) within the crust and formation of giant gas bubbles (Korovkin et al. 2002). Irwin and Barnes (1980) describe the carbon dioxide discharges connected with the seismic activity. They claim that CO<sub>2</sub> discharges may indicate the high pore pressure in the crust and potential seismic regions. Such discharges can initiate acoustic gravity wave generation. The CO<sub>2</sub> discharges have regular character at tectonic faults as a result of thermal crustal anomalies but sometimes they are not observed. In this case, helium-enriched nitrogen is registered in seismic faults (Toutain and Baurbon 1999). The large flows of gas can carry with them other substances that are formed during the morphology transformation process before the earthquake in the form of aerosols. Their presence in the volcano fumaroles is well established (Taran et al. 2001) but aerosol measurements in the seismically active zones are more complicated due to the mosaic character of the gas emanation in the seismic zones and the uncertainty of aerosol origin in gas probes.

According to Toutain and Baurbon (1999), the helium emanating from the crust has a deeper origin in comparison with radon and can indicate the uprising of magma. The <sup>3</sup>He/<sup>4</sup>He isotope ratio permits us to distinguish between atmospheric, crustal and mantle origin of helium.

The other gases such as H<sub>2</sub>, CH<sub>4</sub>, aromatic hydrocarbons are also registered at tectonic faults.

The emanation of volatile metals such as Hg, As, Sb at tectonic faults reported by some authors (Sugisaki et al. 1980; King et al. 1993; Klusman 1993) is also of interest because the metallic ions play a specific role in the developed mechanism of seismo-ionospheric coupling. The emanation of metallic aerosols in seismically active areas was reported also by Alekseev et al. (1995).

### 1.2.4 Anomalous Electric Field

Earthquake preparation is usually accompanied by electromagnetic phenomena in different frequency bands starting from DC up to VHF radio emissions (Hayakawa 1999). Due to the ability of electromagnetic emissions to propagate in the ambient environment, these emissions are registered at different distances from the earthquake epicenter. But one phenomenon, namely the anomalous vertical constant electric field is registered just within the area of the earthquake preparation. This phenomenon was first registered in 1924 by Prof. Chernyavsky (1955). In April 1924 their expedition arrived at Dzhelal-Abad in Kirgizia to study atmospheric electricity. Prof. Chernyavski describes this in the following way: "During the day, when the behavior of our device struck us, the sky was clear. But the equipment with all due evidence demonstrated – electric storm got up in the at-

mosphere with an extremely high potential. What exactly, we were not able to detect because the device arrow went out of the scale limit immediately. And four hours later the Earth yawned. I thought at that time, maybe, the earthquake was the reason of the anomalous state of the atmospheric electric field". The epicentral distance was 120 km, and the earthquake magnitude was 4.5.

We can mention also the early measurements of anomalous atmospheric electric field before earthquakes by Bonchkovsky (1954) and Kondo (1968). The more recent measurements (Hao 1988; Nikiforova and Michnovski 1995; Vershinin et al. 1999; Hao et al. 2000) with modern techniques confirming the early results. To discuss them more definitely, let's look at the examples of anomalous electric field registration presented in Fig. 1.10. Usually, in fair weather conditions the atmospheric electric field is of the order of 100 V/m and directed down to the ground (the atmospheric electricity physics will be discussed below), which is clearly seen in Fig. 1.10 (top left panel, continuous bold line). Some daily variations within the limit of 50 V/m can be observed. But one day before the strong earthquake in the Carpathian mountains (30.08.86,  $M=6.9$ ) the picture changed drastically (Nikiforova and Michnovski 1995). One can observe the increase of the electric field up to the value of 770 V/m, and even a flip of the natural electric field direction at 04 LT to  $-280$  V/m. The peak-to-peak variation of the electric field exceeds 1 kV/m. It should be mentioned also that the electric field measurements were conducted in Poland, 700 km apart from the earthquake epicenter what implies the large size of the earthquake preparation zone, and consequently, the large earthquake magnitude.

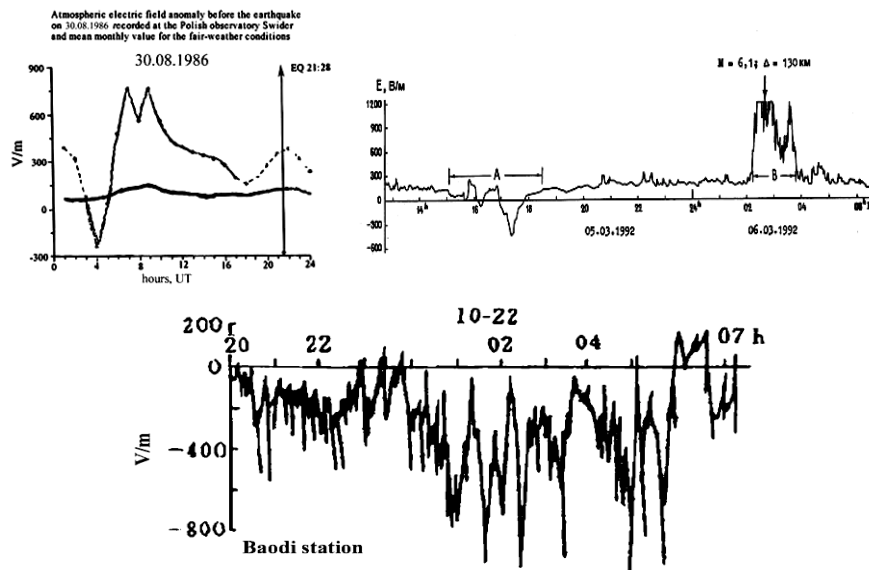


**Fig. 1.10** Examples of anomalous electric field registration before strong earthquakes (Nikiforova and Michnowski 1995; Vershinin et al. 1999; Hao et al. 2000)

A similar picture is observed in Kamchatka records (Vershinin et al. 1999, Fig. 1.10 top right panel) for the earthquake with magnitude 6.1 at the distance 130 km from the epicenter. Here one can see again the increase of electric field in the natural direction up to the device saturation over 1 kV/m, and an electric field flip with the negative value near  $-500$  V/m with the peak-to-peak span over 1.5 kV/m. A slightly different picture is observed in Chinese records (Hao et al. 2000, Fig. 1.10, bottom panel). The prevailing negative electric field is observed in close to epicenter records (38 and 130 km), and increased electric field of natural direction at the far measurement point (320 km) for the earthquake with magnitude 4.7. And again, the peak-to-peak value of the anomalous electric field exceeds 1 kV/m.

Summarizing the aforesaid, we can state that before the strong earthquakes in fair weather conditions the anomalies of atmospheric electric field have been observed in the form of electric field increase up to values exceeding sometimes 1 kV/m, electric field overturn with negative values of electric field also reaching sometimes  $-1$  kV/m. The peak-to-peak difference between the extremes of the positive and negative values of electric field usually exceeds 1 kV/m. The area occupied by the anomalous electric field is very large and for earthquakes with magnitude close to 7 is at least 1,400 km in diameter. According to Hao et al. (2000) the time in advance of the anomalous electric field appearance could be more than one month (the maximum value indicated in Table 1 of their paper is 38 days).

### 1.2.5 Earthquake Preparation Zone

The conception of the earthquake preparation zone was developed by different authors (Dobrovolsky et al. 1979; Keilis-Borok and Kossobokov 1990; Bowman et al. 1998). In general words, this is an area, where the local deformations connected with the source of the future earthquake are observed. Naturally, the deformations imply the changes of the crust properties, which could be measured by different techniques. First of all the deformations are accompanied by the strain storing, so the mechanical properties could be measured by strain meters, dephormographs and tilt meters (Yoshihisa et al. 2002), as well as by a recently developed GPS technique (Kostoglodov et al. 2003). According to dilatation theory (Scholz et al. 1973; Myachkin et al. 1975) formation of the cracks happens within the preparation zone and will be accompanied by changes in the seismic waves velocity, density, electric resistivity, ground water level, and geochemical precursors. All these changes can be monitored experimentally. All these physical and chemical changes within the earthquake preparation zone create the physical basis for the earthquake prediction (Rikitake 1976; Mogi 1985; Sobolev 1993). Regardless of the fact that dilatation theory is not more widely accepted and self-organized criticality became a more common approach of the seismologists, the earthquake preparation zone (or earthquake activation zone in other publications) remains commonly accepted with the same scale parameters as for dilatation (Kossobokov et al. 2000).

Ionospheric Precursors of Earthquakes

Pulinets, S.; Boyarchuk, K.

2005, XIII, 315 p., Hardcover

ISBN: 978-3-540-20839-6